

Fully 4-D Dynamic Cardiac SPECT Image Reconstruction Using Spatiotemporal B-Spline Voxelization

Bryan W. Reutter, *Senior Member, IEEE*, Grant T. Gullberg, *Fellow, IEEE*, Rostyslav Boutchko, Karthikayan Balakrishnan, Elias H. Botvinick, and Ronald H. Huesman, *Fellow, IEEE*

Abstract—We developed fully 4-D penalized least-squares reconstruction methods that use overlapping multiresolution B-splines to represent radiopharmaceutical distributions that vary smoothly in space and time in human dynamic cardiac SPECT images. This approach does not require segmentation, and improves signal-to-noise and increases computational efficiency compared to methods based on small, non-overlapping cube-shaped voxels and rectangular time windows. The support of spatial B-splines was extended into the time dimension to obtain estimates of time-activity curves directly from projections for a human dynamic Tc-99m -sestamibi cardiac SPECT/CT study. Projection data were acquired in 1-sec time frames with an angular step of 5 deg per frame on a GE Millennium VH Hawkeye SPECT/CT scanner. Attenuation and depth-dependent collimator response were modeled, but not scatter. The 4-D B-splines were piecewise trilinear in space and piecewise quadratic in time. The splines were organized on a 3-D spatial grid that provided uniform sampling of 17.7 mm in each dimension, and on a 1-D temporal grid that provided nonuniform sampling intervals of 0–4, 4–15, 15–48, and 48–144 sec during the first two gantry rotations. The use of nonuniform time sampling with 4-D B-splines that varied quadratically in time yielded smooth time-activity curves that captured the relatively fast rise and fall of tracer in the right and left blood chambers, as well as uptake and retention of tracer in the left ventricular myocardium. These methods can also be applied to dynamic PET.

Index Terms—Dynamic SPECT, SPECT/CT, fully four-dimensional reconstruction, spatiotemporal B-splines, penalized least-squares

I. INTRODUCTION

THIS work builds on our most recent work in fully 3-D single-photon emission computed tomography (SPECT) image reconstruction [1], [2] by extending the support of spatial B-spline basis functions into the time dimension to obtain estimates of time-activity curves for the left ventricular blood pool and myocardium directly from projections for a human dynamic Tc-99m -sestamibi cardiac SPECT/CT study.

This work was supported by the National Institutes of Health of the U. S. Department of Health and Human Services under grants R01-HL50663 and R01-HL71253, and by the Director, Office of Science, Office of Biological and Environmental Research, Medical Sciences Division of the U. S. Department of Energy under contract DE-AC03-76SF00098.

B. W. Reutter, G. T. Gullberg, R. Boutchko, and R. H. Huesman are with the Department of Medical Imaging Technology, Lawrence Berkeley National Laboratory, One Cyclotron Road, Berkeley, CA 94720, USA (e-mail: bwreutter@lbl.gov).

K. Balakrishnan is with Philips Medical Systems, Cleveland, OH, USA.

E. H. Botvinick is with the Departments of Radiology and Medicine, University of California, San Francisco, CA 94143, USA.

Unlike an approach that we investigated earlier [3]–[10], this approach does not require segmentation of the myocardial blood pool and tissue volumes in the projected field of view. The overlapping 4-D B-spline basis functions are piecewise trilinear in space and piecewise quadratic in time. Signal-to-noise and computational efficiency are improved, compared to conventional methods based on small, non-overlapping, cube-shaped voxels and rectangular time windows.

Spatiotemporal B-spline coefficients that tend to have negative values are identified with use of an iterative algorithm that converges quickly. These coefficients are then constrained to stay near zero with use of a quadratic penalty that penalizes nonzero contributions to the projection data model. Use of the penalty dramatically reduces image noise while maintaining relatively good spatial and temporal resolution.

The use of nonuniform time sampling with 4-D B-splines that vary quadratically in time yields smooth time-activity curves that capture the relatively fast rise and fall of radiotracer in the right and left blood chambers, as well as uptake and retention of radiotracer in the left ventricular myocardium. These methods can also be applied to dynamic PET.

II. METHODS

A. Regularized Least-Squares Reconstruction with Negativity Penalty

A dynamic SPECT projection data model that relates detected events to a 4-D spatiotemporal B-spline representation of a time-varying radiotracer distribution can be written as

$$\mathbf{p} = \mathbf{Fa}, \quad (1)$$

where \mathbf{p} is an I -element column vector of modeled dynamic projection data values, \mathbf{F} is an $I \times M$ system matrix, \mathbf{a} is an M -element column vector of B-spline coefficients, I is the total number of projection measurements acquired by the SPECT detector(s), and M is the number of 4-D B-spline basis functions that span the space and time to be reconstructed. The system matrix \mathbf{F} incorporates the spline model for time variation of the radiotracer distribution, as well as physical effects such as attenuation, depth-dependent collimator response, and scatter that affect detection of gamma rays emitted by the radiotracer distribution.

At the outset, the least-squares criterion to be minimized, χ^2 , is simply the sum of squared differences between the

measured projections, \mathbf{p}^* , and the modeled projections:

$$\chi^2 = (\mathbf{p}^* - \mathbf{F}\mathbf{a})^T(\mathbf{p}^* - \mathbf{F}\mathbf{a}), \quad (2)$$

where the superscript “T” denotes the matrix transpose. Minimizing the criterion χ^2 yields an estimate, $\hat{\mathbf{a}}$, of coefficients for the 4-D B-spline basis functions that represent the time-varying radiotracer distribution:

$$\hat{\mathbf{a}} = (\mathbf{F}^T\mathbf{F})^{-1}\mathbf{F}^T\mathbf{p}^*. \quad (3)$$

The corresponding minimum value for the criterion χ^2 is

$$\chi_{\min}^2 = (\mathbf{p}^* - \mathbf{F}\hat{\mathbf{a}})^T(\mathbf{p}^* - \mathbf{F}\hat{\mathbf{a}}). \quad (4)$$

Generally speaking, some of the coefficients in the estimate $\hat{\mathbf{a}}$ may have relatively large negative values, particularly for very noisy dynamic projection data measurements \mathbf{p}^* . To constrain these non-physiological values we wish to add a term to the criterion χ^2 that penalizes negative values. Insight into what a reasonable penalty term might be can be obtained by expressing χ^2 in terms of its minimum value:

$$\begin{aligned} \chi^2 &= (\mathbf{p}^* - \mathbf{F}\hat{\mathbf{a}})^T(\mathbf{p}^* - \mathbf{F}\hat{\mathbf{a}}) \\ &= [(\mathbf{p}^* - \mathbf{F}\hat{\mathbf{a}}) - \mathbf{F}(\mathbf{a} - \hat{\mathbf{a}})]^T[(\mathbf{p}^* - \mathbf{F}\hat{\mathbf{a}}) - \mathbf{F}(\mathbf{a} - \hat{\mathbf{a}})] \\ &= \chi_{\min}^2 - 2(\mathbf{p}^* - \mathbf{F}\hat{\mathbf{a}})^T\mathbf{F}(\mathbf{a} - \hat{\mathbf{a}}) + (\mathbf{a} - \hat{\mathbf{a}})^T\mathbf{F}^T\mathbf{F}(\mathbf{a} - \hat{\mathbf{a}}) \\ &= \chi_{\min}^2 + (\mathbf{a} - \hat{\mathbf{a}})^T\mathbf{F}^T\mathbf{F}(\mathbf{a} - \hat{\mathbf{a}}). \end{aligned} \quad (5)$$

Note that the term in (5) that is linear with respect to $(\mathbf{a} - \hat{\mathbf{a}})$ vanishes because the model error $\mathbf{p}^* - \mathbf{F}\hat{\mathbf{a}}$ lies in the null space of the backprojection operator \mathbf{F}^T .

Examining (5), one sees that deviation of \mathbf{a} away from $\hat{\mathbf{a}}$ increases χ^2 by an amount $(\mathbf{a} - \hat{\mathbf{a}})^T\mathbf{F}^T\mathbf{F}(\mathbf{a} - \hat{\mathbf{a}})$. To mimic this effect for purposes of constraining negative values, we now define the criterion, ψ^2 , which adds a term to χ^2 that penalizes deviations of certain elements of \mathbf{a} away from zero:

$$\psi^2 = \chi^2 + \mathbf{a}^T\mathbf{N}\mathbf{F}^T\mathbf{F}\mathbf{N}\mathbf{a}, \quad (6)$$

where the $M \times M$ matrix \mathbf{N} is a diagonal matrix whose (m, m) -th element is one if the penalty is to be applied to the m -th element of \mathbf{a} , or is zero if the penalty is not to be applied to the m -th element of \mathbf{a} . In essence, the additional term penalizes nonzero contributions to the dynamic projection data model resulting from the forward projection, $\mathbf{F}\mathbf{N}\mathbf{a}$, of spatiotemporal spline basis functions whose coefficients are flagged by the diagonal elements of \mathbf{N} .

Thus, if the matrix \mathbf{N} is properly defined the criterion ψ^2 tends to drive coefficients of $\hat{\mathbf{a}}$, which would be negative without the penalty, closer to zero. Note that there is no arbitrary multiplicative scaling factor (*i.e.*, hyperparameter) applied to the penalty term, as the term appears to be already properly scaled with respect to χ^2 by virtue of (5).

Given the matrix \mathbf{N} , the criterion ψ^2 is minimized by

$$\tilde{\mathbf{a}} = (\mathbf{F}^T\mathbf{F} + \mathbf{N}\mathbf{F}^T\mathbf{F}\mathbf{N})^{-1}\mathbf{F}^T\mathbf{p}^*. \quad (7)$$

The matrix \mathbf{N} can be defined and a penalized least-squares estimate $\tilde{\mathbf{a}}$ can be obtained in a few iterations as follows:

- 1) Initialize \mathbf{N} to be a zero matrix.

- 2) Minimize the criterion χ^2 in eqn. (2) via direct matrix inversion [eqn. (3)] to obtain the estimate $\hat{\mathbf{a}}$.
- 3) Set diagonal elements of \mathbf{N} that correspond to negative elements of $\hat{\mathbf{a}}$ to one.
- 4) Minimize the criterion ψ^2 in eqn. (6) via direct matrix inversion [eqn. (7)] to obtain an estimate $\tilde{\mathbf{a}}$.
- 5) Set diagonal elements of \mathbf{N} that correspond to negative elements of $\tilde{\mathbf{a}}$ to one, if they are not already one. Once a diagonal element of \mathbf{N} has been set to one, it should remain at one even if the corresponding element in $\tilde{\mathbf{a}}$ swings positive.
- 6) Repeat steps 4 and 5 until the matrix \mathbf{N} does not change. The resulting estimate $\tilde{\mathbf{a}}$ is the “final” estimate.

For the fully 4-D dynamic cardiac SPECT patient image reconstruction described in Section II-B1, the matrix \mathbf{N} converged in 7 iterations of steps 4 and 5. Inversion of the symmetric, positive definite matrices in eqns. (3) and (7) can be accomplished relatively quickly and robustly with use of Cholesky decomposition [11].

B. Reconstruction of a Dynamic ^{99m}Tc -Sestamibi Cardiac SPECT/CT Patient Study

Emission data were acquired with use of parallel-hole collimators on a dual-head GE Millennium VH Hawkeye SPECT/CT scanner. A 30 min dynamic scan was performed, with the patient’s arms down for comfort, subsequent to pharmacologically induced stress as part of a rest/stress protocol. During the scan, the gantry performed 24 360-deg rotations, acquiring 72 views per head per rotation at 1 sec per view. Projections at each view were binned into frames of 64×64 pixels, with pixel size $8.84 \text{ mm} \times 8.84 \text{ mm}$. Images were reconstructed from projections of the heart obtained in 64 (transverse) $\times 9$ (axial) subframes of the data. An X-ray CT scan was performed with use of the integrated Hawkeye system to obtain an attenuation map. Attenuation and depth-dependent collimator response were modeled, but not scatter.

1) Fully 4-D Reconstruction of Dynamic Early Data: A dynamic image volume was reconstructed from data in 64×9 subframes of the 144 dynamic views per head acquired during the first two gantry rotations. These early data contained 0.8 million counts. The 4-D B-splines were piecewise trilinear in space and piecewise quadratic in time. The splines were organized on a $31 \times 31 \times 5$ 3-D spatial grid that provided uniform sampling of $17.7 \text{ mm} \times 17.7 \text{ mm} \times 17.7 \text{ mm}$ along the x -, y -, and z -axes, respectively, where x and y are transverse coordinates and z is the axial coordinate; and on a 1-D temporal grid that provided nonuniform sampling intervals of 0–4, 4–15, 15–48, and 48–144 sec during the first two gantry rotations (Fig. 1). Post-reconstruction smoothing was performed so that each point in an image represents the average intensity in a $26.5 \text{ mm} \times 26.5 \text{ mm} \times 26.5 \text{ mm}$ volume centered at that point.

2) Fully 3-D Reconstruction of Summed Late Data: A static image volume was reconstructed from data in 64×9 subframes of the 72 summed views acquired during the last 22 gantry

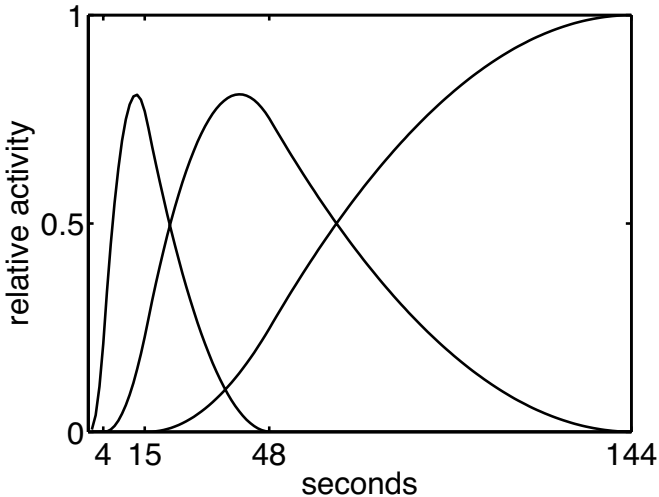


Fig. 1. Piecewise quadratic temporal B-spline basis functions used to reconstruct data from the first two gantry rotations.

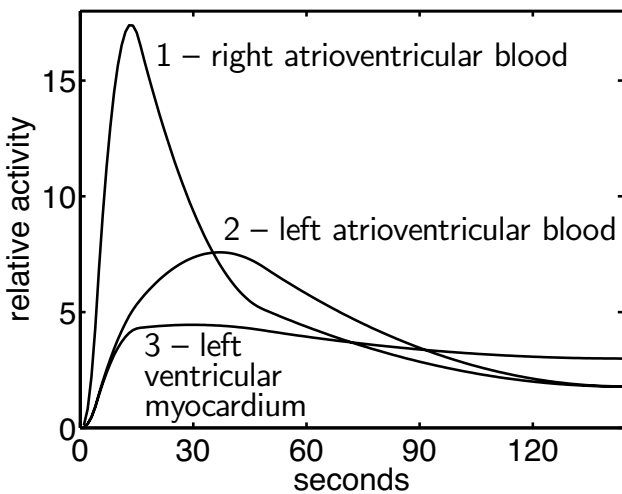


Fig. 2. Time-activity curves estimated directly from projections. These curves correspond to volumes of interest centered at the crosses labeled “1”, “2”, and “3” in Fig. 3.

rotations. These late data contained 6.8 million counts. The 3-D B-splines were piecewise trilinear in space and were organized on a $63 \times 63 \times 5$ 3-D spatial grid that provided uniform sampling of $8.84 \text{ mm} \times 8.84 \text{ mm} \times 17.7 \text{ mm}$ along the x -, y -, and z -axes, respectively. Post-reconstruction smoothing was performed so that each point in an image represents the average intensity in a $17.7 \text{ mm} \times 17.7 \text{ mm} \times 17.7 \text{ mm}$ volume centered at that point.

III. RESULTS

For the fully 4-D dynamic ^{99m}Tc -sestamibi cardiac SPECT reconstruction, the use of nonuniform time sampling with 4-D B-splines that varied quadratically in time yielded smooth time-activity curves (Fig. 2) that captured the relatively fast rise and fall of radiotracer in the right and left blood chambers, as well as uptake and retention of radiotracer in the left

ventricular myocardium.

Fig. 3 shows time samples of a transaxial mid-ventricular cross-section through the fully 4-D dynamic reconstruction. Radiotracer is seen primarily in the right ventricular blood pool at 15 sec and 30 sec post-injection (Figs. 3a and 3b, cross labelled “1”). At 45 sec and 60 sec, radiotracer is seen primarily in the left ventricular blood pool (Figs. 3c and 3d, cross labelled “2”). Retention of radiotracer in the left ventricular myocardium is evident at 90 sec and 120 sec (Figs. 3e and 3f, cross labelled “3”), as well as in the fully 3-D reconstruction of late summed data (Fig. 3g). The smoothed attenuation map acquired by the Hawkeye CT system is shown in Fig. 3h.

Using a dual-processor 2.5-GHz PowerPC G5 Macintosh with 8 GB of memory and MATLAB software, the fully 4-D reconstruction of the dynamic early data took 46 cpu-min, while the fully 3-D reconstruction of the summed late data took 8.4 cpu-min. A large part of the computational time was spent calculating $\mathbf{F}^T \mathbf{F}$.

IV. DISCUSSION

To the best of our knowledge, no other group has successfully developed methods to reconstruct the rise and fall of the blood input function from dynamic cardiac SPECT data acquired with a gantry rotating at less than one revolution per minute (*e.g.*, at the speed of 5/6 rpm used for the patient study presented here).

Future work includes implementation of spatial modeling with tri-quadratic B-splines, which are smoother and more circularly symmetric than trilinear B-splines. We are also working to improve the statistical efficiency of fully 4-D reconstruction with use of penalized weighted least-squares inversion or iterative maximization of Poisson likelihood. These methods can also be applied to dynamic PET.

ACKNOWLEDGMENT

This work was supported by the National Institutes of Health of the U. S. Department of Health and Human Services under grants R01-HL50663 and R01-HL71253, and by the Director, Office of Science, Office of Biological and Environmental Research, Medical Sciences Division of the U. S. Department of Energy under contract DE-AC03-76SF00098.

This document was prepared as an account of work sponsored by the United States Government. While this document is believed to contain correct information, neither the United States Government nor any agency thereof, nor The Regents of the University of California, nor any of their employees, makes any warranty, express or implied, or assumes any legal responsibility for the accuracy, completeness, or usefulness of any information, apparatus, product, or process disclosed, or represents that its use would not infringe privately owned rights. Reference herein to any specific commercial product, process, or service by its trade name, trademark, manufacturer, or otherwise, does not necessarily constitute or imply its endorsement, recommendation, or favoring by the United States Government or any agency thereof, or The Regents of the University of California. The views and opinions of authors

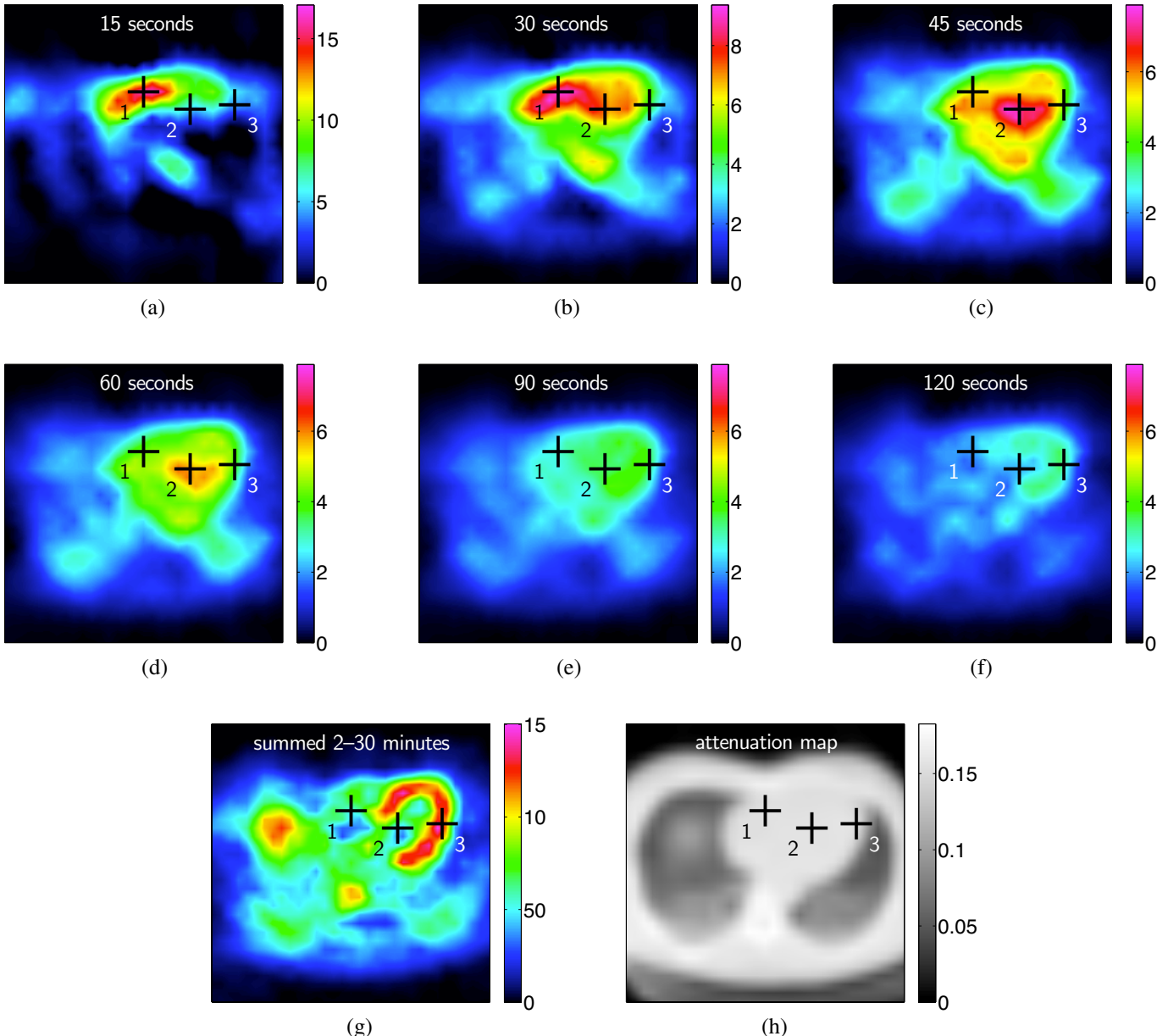


Fig. 3. Fully 4-D dynamic ^{99m}Tc -sestamibi cardiac SPECT reconstruction showing time samples of a transaxial mid-ventricular cross-section. Radiotracer is seen primarily in the right ventricular blood pool at (a) 15 sec and (b) 30 sec post-injection (cross labelled “1”); in the left ventricular blood pool at (c) 45 sec and (d) 60 sec (cross labelled “2”); and in the left ventricular myocardium at (e) 90 sec, (f) 120 sec, and (g) 2–30 min (cross labelled “3”). The smoothed attenuation map acquired by the Hawkeye CT system is shown in (h). Time-activity curves for volumes of interest centered at the labelled crosses are shown in Fig. 2.

expressed herein do not necessarily state or reflect those of the United States Government or any agency thereof or The Regents of the University of California.

REFERENCES

- [1] B. W. Reutter, G. T. Gullberg, A. Sitek, R. Boutchko, E. H. Botvinick, and R. H. Huesman, “Modeling spatial smoothness in fully 3-D SPECT image reconstruction using multiresolution B-splines,” in *2006 IEEE Nuclear Science Symposium and Medical Imaging Conference Record*, B. Philips, Ed., 2006, pp. 1757–1761.
- [2] B. W. Reutter, G. T. Gullberg, R. Boutchko, K. Balakrishnan, E. H. Botvinick, and R. H. Huesman, “Regularized least-squares SPECT image reconstruction using multiresolution spatial B-splines and a negativity penalty,” in *Proceedings of the 9th International Conference on Fully 3D Image Reconstruction in Radiology and Nuclear Medicine*, M. Kachelrieß and F. Beekman, Eds., 2007, pp. 305–308.
- [3] R. H. Huesman, B. W. Reutter, G. L. Zeng, and G. T. Gullberg, “Kinetic parameter estimation from SPECT cone-beam projection measurements,” *Phys Med Biol*, vol. 43, no. 4, pp. 973–982, 1998.
- [4] B. W. Reutter, G. T. Gullberg, and R. H. Huesman, “Kinetic parameter estimation from attenuated SPECT projection measurements,” *IEEE Trans Nucl Sci*, vol. 45, no. 6, pp. 3007–3013, 1998.
- [5] ———, “Kinetic parameter estimation from dynamic cardiac patient SPECT projection measurements,” in *1998 IEEE Nuclear Science Symposium and Medical Imaging Conference Record*, R. Sudharsanan, Ed., 1999, pp. 1953–1958.
- [6] ———, “Direct least-squares estimation of spatiotemporal distributions from dynamic SPECT projections using a spatial segmentation and temporal B-splines,” *IEEE Trans Med Imag*, vol. 19, no. 5, pp. 434–450, 2000.

- [7] ——, “Effects of temporal modelling on the statistical uncertainty of spatiotemporal distributions estimated directly from dynamic SPECT projections,” *Phys Med Biol*, vol. 47, no. 15, pp. 2673–2683, 2002.
- [8] ——, “Accuracy and precision of compartmental model parameters obtained from directly estimated dynamic SPECT time-activity curves,” *IEEE Trans Nucl Sci*, vol. 51, no. 1, pp. 170–176, 2004.
- [9] ——, “Fully 4-D direct joint estimation of compartmental models and blood input function from dynamic SPECT projections,” in *Proceedings of the 7th International Conference on Fully 3D Image Reconstruction in Radiology and Nuclear Medicine*, Y. Bizais, Ed., 2003, pp. Mo-PM3-1/1-4.
- [10] B. W. Reutter, S. Oh, G. T. Gullberg, and R. H. Huesman, “Improved quantitation of dynamic SPECT via fully 4-D joint estimation of compartmental models and blood input function directly from projections,” in *2005 IEEE Nuclear Science Symposium and Medical Imaging Conference Record*, B. Yu, Ed., 2005, pp. 2337–2341.
- [11] W. H. Press, S. A. Teukolsky, W. T. Vetterling, and B. P. Flannery, *Numerical Recipes in C: The Art of Scientific Computing*, 2nd ed. Cambridge, England: Cambridge University Press, 1992.